Int. J. Heat Mass Transfer. Vol. 12, pp. 365–369. Pergamon Press 1969. Printed in Great Britain

SHORTER COMMUNICATIONS

FREE CONVECTION FROM A PLANE VERTICAL SURFACE WITH A NON-HORIZONTAL LEADING EDGE

E. M. SPARROW and R. B. HUSAR

Department of Mechanical Engineering, University of Minnesota, Minneapolis, Minnesota

(*Received* 2 *May* 1968)

NOMENCLATURE

- c_p, specific heat at constant pressure;
- g, acceleration of gravity;
- h, local heat-transfer coefficient, equation (14);
- k, thermal conductivity;
- Nu, local Nusselt number, equation (14);
- Gr, Grashof number, equation (14);
- Pr, Prandtl number;
- Q, overall rate of heat transfer;
- q, local rate of heat transfer per unit area;
- R_1, ratio of net shear stress terms, equation (6);
- R_2, ratio of net heat conduction terms, equation (6);
- T, temperature;
- T_∞, ambient temperature;
- T_w, wall temperature;
- u, vertical velocity component;
- u_1, velocity scaling function, equation (7);
- v, transverse velocity component;
- x, vertical coordinate;
- y, transverse coordinate (normal to plate);
- z, spanwise coordinate.

Greek symbols

- β, coefficient of thermal expansion;
- δ, boundary-layer thickness;
- ζ, function describing shape of leading edge;
- μ, viscosity;
- ν, kinematic viscosity;
- ξ, local vertical height above leading edge;
- ρ, density.

INTRODUCTION

FREE convection heat transfer from a plane vertical surface has been studied exhaustively during the last two decades. These investigations have examined a wide range of factors such as thermal boundary conditions, fluid property variations, interactions with forced flows, surface mass transfer, low Grashof number effects, and so forth. One of the conditions common to all such studies is that the leading edge of the plate is horizontal, this condition being imposed to help insure two-dimensional velocity and temperature fields. On the other hand, in practice, situations are frequently encountered where the leading edge is not horizontal. Such a configuration admits three-dimensional velocity and temperature fields, along with the possibility that all three velocity components may be non-zero.

The present investigation is concerned with free convection from a plane vertical surface, the leading edge of which is not horizontal. In the first phase of the study, experiments were performed with a view to establishing the nature of the velocity field, specifically with respect to the existence of a spanwise velocity component. The experiments involved the application of a flow visualization technique by which the flow field is made visible by local changes of color of the fluid itself, the color change resulting from a change in pH. The experimental findings facilitate the development of a quasi two-dimensional analytical model, which is then applied to provide free convection heat transfer results for vertical plates with non-horizontal leading edges.

EXPERIMENTAL APPARATUS

The plane vertical surfaces that were employed in the experimental studies are pictured in Fig. 1(a) through 1(e). The first of these has a horizontal leading edge and is used as a standard. The other plates have non-horizontal leading edges. The leading edge of the second plate (Fig. 1(b)) is semi-circular in form, with a diameter which is approximately equal to the plate width. The third and fourth plates (Figs. 1(c) and 1(d), respectively) have triangular leading edges, with vertex angles of 90° and 60° respectively. The last test surface, Fig. 1(e) is the same plate that was shown in Fig. 1(a), but is now tilted.

The overall heights (from lowest to highest point) of all the test surfaces are 20 cm, and the widths are 10 cm. The test surfaces were fabricated from copper plate, $4\frac{1}{2}$ mm in thickness.

Each one of the test surfaces was mounted in a frame made of $\frac{4}{3}$ mm-thick Plexiglass. The test surface and its frame formed a vertical wall that spanned the width of the test chamber. In all cases, the frame extended 5 cm below the lowest point of the test plate, the lower edge of the frame resting on the floor of the test chamber. The test plate-Plexiglass units were interchangeably installed at one end of the test chamber. Slots in the chamber wall facilitated vertical positioning of the test surfaces. The chamber itself was a Plexiglass tank which provided a fluid environment whose horizontal dimensions were 26 × 25 cm (respectively normal and parallel to the test plate). The chamber was filled to a height of approximately 35 cm with distilled water. Thus, under operating conditions, the water environment extended 10 cm above the uppermost point of the plate and 5 cm below the lowermost point.

Heating of each of the test plates was accomplished by electrical means. Nichrome heating wire ($\frac{1}{2}$ mm dia.) was cemented to the rear surface of the plate. The wire was arranged in back and forth horizontal segments, with 76 such segments covering the overall height of the plate. Temperature was measured by a pair of copper-constantan thermocouples soldered into holes drilled into the rear surface. The temperature of the fluid environment was read from a precision thermometer. Generally, the temperature difference between the test plate and the fluid was about 10°F.

The flow visualization technique employed here is an extension of that described by Baker [1]. Thymol blue, a pH indicator†, is added to the water in an amount approximately 0·01 per cent by weight. The solution is titrated to the end point (pH ~ 8) with sodium hydroxide. Then, by the addition of hydrochloric acid, the solution is made acidic and yellow in color. When a small D.C. voltage (~10 V) from a dry-cell source is impressed between the test surface (negative electrode) and a copper billet (positive electrode) remotely situated in the fluid environment, there is a proton transfer reaction at the former. As a result, there is a change in pH of the fluid at the surface of the electrode (acid to base), with a corresponding change in color from yellow to blue. This process does not give rise to density differences within the fluid, so no extraneous buoyancy forces are induced. The thus-created "dye" faithfully follows the motions of the fluid.

If the entire test surface were to function as an electrode, it would, under steady-state operating conditions, be blanketed by a film of upward-moving blue fluid. Aside from this gross upward motion, no other details of the flow field would be discernible. To facilitate more detailed observation of the flow field (specifically, the presence or absence of spanwise velocity components), the plate surface was spray coated with a thin electrically insulating layer. Only at five discrete locations along the leading edge of each plate was the surface left uncoated (see Figs. 1(a) through 1(e)). "Dye" is formed only at these discrete locations and is carried upward by the free convection motion. Any departure of these dye strands from the vertical would signal the presence of spanwise velocity components in the boundary layer.

The surface coating used in the present tests was a white enamel paint. This choice was made with a view to providing higher contrast for the blue "dye" stream to facilitate photography. The photographs of the flow patterns were taken on Kodak tri-X film with an Exakta camera which looked head-on at the test surface through the Plexiglass wall of the chamber. Yellow photoflood lights were used to further highlight the flow field. Prints were made on contrast grade F-6 paper.

FLOW FIELD OBSERVATIONS

Attention may first be directed to Fig. 1(a), which shows a vertical plate having a horizontal leading edge. Inspection of the figure shows that the dye strands are straight, vertical lines, as would be expected for this case. Furthermore, the flow field, as evidenced by the dye strands, was completely steady over an indefinite period of time. It is especially interesting to observe that even at the lateral edges of the plate, the characteristics of steady, vertical flow continue to hold, thereby testifying to the minor influence of edge effects on the velocity field. The photographic evidence of Fig. 1(a) confirms the absence of extraneous currents in the fluid environment or other unforseen conditions which might induce spanwise velocities adjacent to the plate surface.

Next, consideration may be given to Figs. 1(b) through 1(e), which show flow field visualizations for vertical plates with non-horizontal leading edges. In all cases, the dye strands are parallel vertical lines, even adjacent to the lateral edges. These flow patterns were absolutely stable and were reproducible at will.

The dye strand patterns of Figs. 1(b) through 1(e) reveal no evidence of the presence of spanwise velocity components. Additional flow visualization studies were performed to affirm this finding. Obstructions were placed in the path of the dye strand, thus causing local separation from the plate surface. Downstream of the reattachment, the dye stripe was vertical and, in fact, coincided with the position of the stripe in the absence of the obstruction. In other tests, fine wires, serving as electrodes, were positioned at various points in the boundary layer. The dye strands formed at these points showed no tendency toward spanwise movement.

On the basis of the just-described flow visualization studies, spanwise velocities appear to be absent, at least within the capabilities of the visualization technique to

† Thymol blue is blue in color when indicating a basic solution and yellow orange in color when indicating an acidic solution.

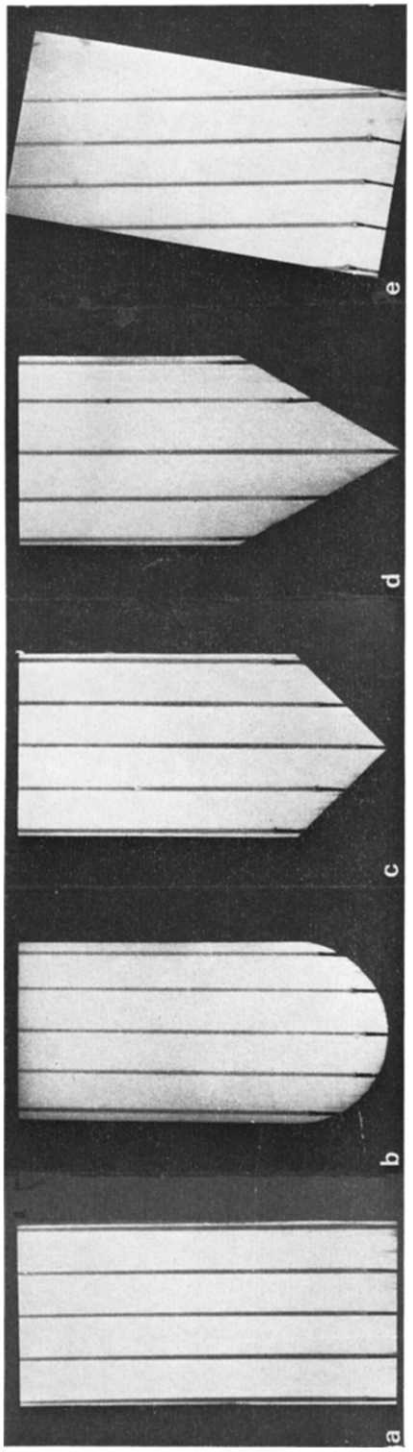

FIG. 1. Flow visualization photographs.

facing page 366

detect such velocities. An estimate suggests that spanwise velocities which are as small as one hundreth of the vertical velocity can be detected. Therefore, if spanwise velocities do exist, they are no greater than one hundreth of the vertical velocity. Thus, in analyzing free convection from a vertical plate with a non-horizontal leading edge, there appears to be ample justification for neglecting the spanwise velocity components.

ANALYSIS

The foregoing finding facilitates the development of a simple analytical model for computing the heat transfer from a vertical plate with a non-horizontal leading edge. Consider a vertical plate with an arbitrary leading edge as pictured schematically in Fig. 2(a). In accordance with the usual convention, the vertical coordinate is denoted by x (here measured from the lowest point of the leading edge) and the coordinate normal to the plate surface is denoted by y. The spanwise coordinate is z.

In terms of these coordinates and taking account of the foregoing experimental finding that the spanwise velocity (i.e. z component) is vanishingly small, the governing conservation equations, in boundary layer form, are

$$\rho\left(u\frac{\partial u}{\partial x}+v\frac{\partial u}{\partial y}\right)=g\beta\rho(T-T_\infty)+\mu\left(\frac{\partial^2 u}{\partial y^2}+\frac{\partial^2 u}{\partial z^2}\right) \quad (1)$$

$$\rho c_p\left(u\frac{\partial T}{\partial x}+v\frac{\partial T}{\partial y}\right)=k\left(\frac{\partial^2 T}{\partial y^2}+\frac{\partial^2 T}{\partial z^2}\right) \quad (2)$$

$$\frac{\partial u}{\partial x}+\frac{\partial v}{\partial y}=0. \quad (3)$$

These equations differ from the conventional free convection boundary layer equations by the presence of the terms $\partial^2 u/\partial z^2$ and $\partial^2 T/\partial z^2$. The first of these represents the contribution of the spanwise velocity variation to the net shear stress, while the second is the net spanwise heat conduction.

It is of interest to examine the orders of magnitude of these terms. For this purpose, the foregoing conservation equations are rewritten in integral form (for instance, [2]),

$$\frac{\partial}{\partial x}\int_0^\delta \rho u^2\,dy=g\beta\rho\int_0^\delta (T-T_\infty)\,dy-\mu\left(\frac{\partial u}{\partial y}\right)_0+\mu\frac{\partial^2}{\partial z^2}\int_0^\delta u\,dy \quad (4)$$

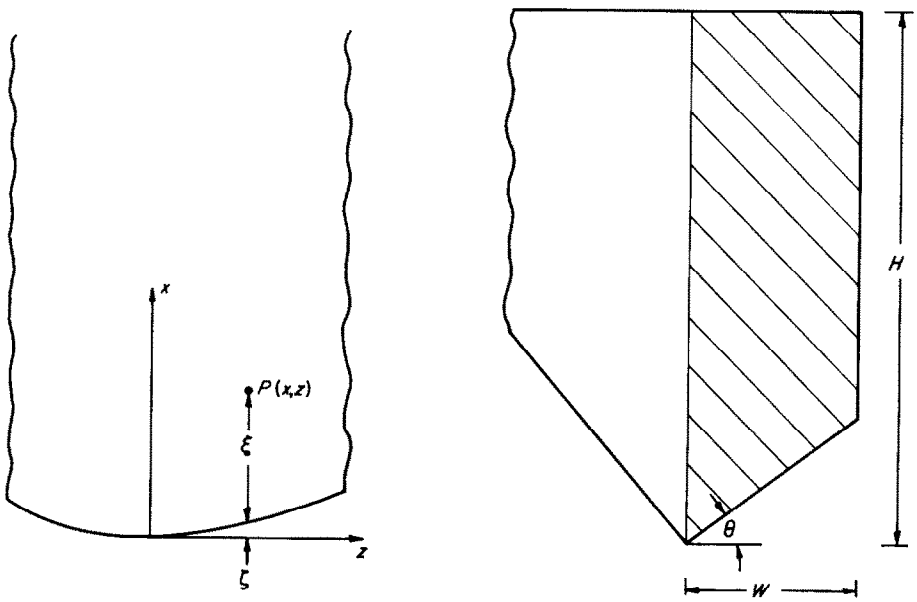

FIG. 2. Diagrams for the analytical development.

$$\frac{\partial}{\partial x}\int_0^\delta \rho c_p u(T - T_\infty)\,dy = -k\left(\frac{\partial T}{\partial y}\right)_0 + k\frac{\partial^2}{\partial z^2}\int_0^\delta (T - T_\infty)\,dy. \quad (5)$$

To appraise the role of the new terms, it is appropriate to consider the ratios

$$R_1 = \frac{\mu\dfrac{\partial^2}{\partial z^2}\displaystyle\int_0^\delta u\,dy}{-\mu\left(\dfrac{\partial u}{\partial y}\right)_0}, \qquad R_2 = \frac{k\dfrac{\partial^2}{\partial z^2}\displaystyle\int_0^\delta (T - T_\infty)\,dy}{-k\left(\dfrac{\partial T}{\partial y}\right)_0}. \quad (6)$$

The ratio R_1 compares, on an integrated basis*, the net shear induced by the spanwise velocity variation with the net shear term for two-dimensional boundary layer flow. The latter is readily identified as the shear stress locally exerted by the plate on the fluid. Similarly, R_2 compares the integrated magnitude† of the net heat conduction in the spanwise direction with that for a two-dimensional thermal boundary layer, the latter corresponding to the heat locally conducted from the plate surface into the fluid.

To proceed with the evaluation of the ratios R_1 and R_2, polynomial forms may be employed for the profiles of u and T. For the isothermal plate (T_w = constant), suitable representations for the profiles are [2],

$$u = u_1\frac{y}{\delta}\left(1 - \frac{y}{\delta}\right)^2, \qquad \frac{T - T_\infty}{T_w - T_\infty} = 1 - \frac{y}{\delta}^2 \quad (7)$$

where

$$u_1 = u_1(x, z), \qquad \delta = \delta(x, z). \quad (7a)$$

The quantity u_1 is a scaling function for the velocity field, while δ is the boundary-layer thickness. The introduction of the polynomial representations into the R ratios yields

$$R_1 = -\frac{\delta}{12u_1}\frac{\partial^2}{\partial z^2}(u_1\delta), \qquad R_2 = \frac{\delta}{6}\frac{\partial^2\delta}{\partial z^2}. \quad (8)$$

† That is, integrated across the boundary layer.

Next, to facilitate the estimation of the magnitudes of R_1 and R_2, it will be assumed that at any point $P(x, z)$, u_1 and δ can be expressed as functions of the local vertical displacement of P from the leading edge. This height, denoted by ξ, is shown in Fig. 2(a). As a first approximation, let

$$u_1 = C_1\xi^{\frac{1}{2}}, \qquad \delta = C_2\xi^{\frac{1}{4}} \quad (9)$$

where the constants C_1 and C_2 and the exponents $\frac{1}{2}$ and $\frac{1}{4}$ are those of two-dimensional free convection boundary layer theory [2].

The spirit in which equations (9) are employed is that of estimating the orders of magnitude of the R ratios and of delineating the conditions for which refined approximations for u_1 and δ are necessary. If, *a postiori*, R_1 and R_2 are found to be very small compared to unity, then further refinements of u_1 and δ are not called for, and it is plausible to accept equations (9) as written.

In terms of the notation of Fig. 2(a), the vertical distance ξ can be expressed in terms of the x, z coordinates as

$$\xi = x - \zeta(z) \quad (10)$$

in which $\zeta = \zeta(z)$ is the equation of the curve representing the shape of the leading edge. Since $\zeta(0) = 0$, then $\xi = x$ when $z = 0$.

The R ratios of equation (8) may now be evaluated by employing equations (9) and (10). The end result of these operations is

$$R_1 = \left(\frac{\delta}{\xi}\right)^2\left[\tfrac{1}{64}(\zeta')^2 + \tfrac{1}{16}\xi\zeta''\right] \quad (11a)$$

$$R_2 = -\left(\frac{\delta}{\xi}\right)^2\left[\tfrac{1}{32}(\zeta')^2 + \tfrac{1}{24}\xi\zeta''\right] \quad (11b)$$

where primes denote differentiation with respect to z.

Inspection of equations (11a) and (11b) indicates that both R_1 and R_2 involve the product of two factors. The first factor is the square of the ratio of the local boundary layer thickness to the local distance from the leading edge. According to boundary layer theory

$$(\delta/\xi)^2 \ll 1. \quad (12)$$

The bracketed quantities in equations (11a) and (11b) depend on the geometry of the leading edge. If the bracketed quantities are of order of magnitude unity or less, then $|R_1| \ll 1$ and $|R_2| \ll 1$. Under these conditions, it would appear plausible to neglect the terms

$$\mu\partial^2/\partial z^2\int_0^\delta u\,dy \quad \text{and} \quad k\,\partial^2/\partial z^2\int_0^\delta (T - T_\infty)\,dy$$

in equations (4) and (5). Once these terms are deleted, the integral momentum and energy equations are essentially restored to their two-dimensional forms, the one difference being that the equations are now applied along lines $z =$ constant. Thus, the problem may be regarded as quasi two-dimensional.

For such a quasi two-dimensional system, the local Nusselt number may be expressed as [2]

$$Nu_\xi = 0{\cdot}508 \frac{Pr^{\frac{1}{2}}}{(0{\cdot}952 + Pr)^{\frac{1}{2}}} Gr_\xi^{\frac{1}{4}} \tag{13}$$

in which

$$\left.\begin{aligned} Nu_\xi &= \frac{h\xi}{k}, \\ Gr_\xi &= \frac{g\beta(T_w - T_\infty)\,\xi^3}{\nu^2}, \\ h &= \frac{q}{T_w - T_\infty}. \end{aligned}\right\} \tag{14}$$

Alternatively, the local Nusselt number can be taken from boundary-layer similarity solutions, that is

$$Nu_\xi = g'(0)\,(Gr_\xi/4)^{\frac{1}{4}} \tag{15}$$

where $g'(0)$ is listed as a function of Prandtl number in Table 1 of [3]†. Therefore, by applying either equation (13) or (15), the local rate of heat transfer at any point on the plate surface can be evaluated. Furthermore, by integrating q over the plate surface, the overall heat-transfer rate Q can be determined.

In view of the highly attractive simplicity of the quasi two-dimensional model, it is appropriate to explore its applicability in representative cases. Consider a plate having a straight (albeit non-horizontal) leading edge as shown in Fig. 2(b). In terms of the nomenclature of the figure,

$$\zeta = z \tan\theta, \qquad \zeta' = \tan\theta, \qquad \zeta'' = 0. \tag{16}$$

With these, R_1 and R_2 become

$$\left.\begin{aligned} R_1 &= \left(\frac{\delta}{\xi}\right)^2 \frac{\tan^2\theta}{64}, \\ R_2 &= -\left(\frac{\delta}{\xi}\right)^2 \frac{\tan^2\theta}{32}. \end{aligned}\right\} \tag{17}$$

† The quantity g'(0) should not be confused with the acceleration of gravity g.

In view of equation (12), $|R_1|$ and $|R_2| \ll 1$ provided that $\tan^2\theta \leqslant 32$ or that $\theta \leqslant 80°$. From the standpoint of practical applications, the just-stated criterion for θ is almost always satisfied. Furthermore, when $\theta \leqslant 45°$, $|R_1| \leqslant \frac{1}{64}(\delta/\xi)^2$ and $|R_2| \leqslant \frac{1}{32}(\delta/\xi)^2$, so that R_1 and R_2 are at least an order of magnitude smaller than $(\delta/\xi)^2$ itself.

These are highly persuasive arguments favoring the use of the quasi two-dimensional model for plates with straight non-horizontal leading edges. If this model is accepted, then the local heat-transfer rate is calculable from equations (13) or (15), while the overall rate of heat transfer Q for a section of plate such as that defined by shading in Fig. 2(b) is

$$\frac{Q}{kW(T - T_\infty)} = \frac{0{\cdot}387\,Pr^{\frac{1}{2}}}{(0{\cdot}952 + Pr)^{\frac{1}{2}}} Gr_H^{\frac{1}{4}} \left[\frac{H}{W} - \frac{H}{W}\left(1 - \frac{W}{H}\tan\theta\right)^{\frac{4}{3}}\right] (\tan\theta)^{-1} \tag{18}$$

which is obtained by integrating equation (13). When θ approaches zero, this expression reduces identically to the conventional equation for the overall heat transfer for a two-dimensional free convection boundary layer flow.

CONCLUDING REMARKS

The flow visualization studies performed during the first phase of this investigation provide persuasive evidence that the spanwise velocities are vanishingly small. As a consequence of deleting the spanwise velocities, the three-dimensionality of the problem enters the governing equations only through additional shear and heat conduction terms. An order of magnitude estimate suggests that, in most physical situations, these terms are negligible compared with the shear and heat conduction terms that appear in the two-dimensional boundary layer equations. Under these conditions, the problem can be treated as quasi two-dimensional.

Although it cannot be asserted that the order of magnitude estimate is strictly rigorous, it is, in the view of the authors, highly plausible.

REFERENCES

1. D. J. Baker, A technique for the precise measurement of small fluid velocities, *J. Fluid Mech.* **26**, 573–575 (1966).
2. E. R. G. Eckert and R. M. Drake, *Heat and Mass Transfer*, McGraw-Hill, New York (1959).
3. A. J. Ede, Advances in free convection, in *Advances in Heat Transfer* (Edited by J. P. Hartnett and T. F. Irvine, Jr.), Academic Press, New York (1967).